

Non-invasive measurement and imaging of tissue iron oxide nanoparticle concentrations *in vivo* using proton relaxometry

T G St Pierre¹, P R Clark¹, W Chua-anusorn¹, A Fleming¹, H Pardoe¹,
G P Jeffrey², J K Olynyk², P Pootrakul³, S Jones⁴, P Moroz²

¹School of Physics, The University of Western Australia, Perth, WA 6009, Australia

²School of Medicine and Pharmacology, The University of Western Australia, Perth, WA 6009, Australia

³Thalassemia Research Center, Institute of Science and Technology for Research and Development, Mahidol University, Bangkok, Thailand

⁴Sirtex Medical Limited, F6/16 Mars Rd, Lane Cove 2066, Sydney, NSW, Australia

Email: stpierre@physics.uwa.edu.au

Abstract. Magnetic nanoparticles and microparticles can be found in biological tissues for a variety of reasons including pathological deposition of biogenic particles, administration of synthetic particles for scientific or clinical reasons, and the inclusion of biogenic magnetic particles for the sensing of the geomagnetic field. In applied magnetic fields, the magnetisation of tissue protons can be manipulated with radiofrequency radiation such that the macroscopic magnetisation of the protons precesses freely in the plane perpendicular to the applied static field. The presence of magnetic particles within tissue enhances the rate of dephasing of proton precession with higher concentrations of particles resulting in higher dephasing rates. Magnetic resonance imaging instruments can be used to measure and image the rate of decay of spin echo recoverable proton transverse magnetisation (R_2) within tissues enabling the measurement and imaging of magnetic particle concentrations with the aid of suitable calibration curves. Applications include the non-invasive measurement of liver iron concentrations in iron-overload disorders and measurement and imaging of magnetic particle concentrations used in magnetic hyperthermia therapy. Future applications may include the tracking of magnetically labelled drugs or biomolecules and the measurement of fibrotic liver damage.

1. Introduction

Magnetic iron oxide nanoparticles can occur naturally in biological tissue or can be introduced for scientific or clinical reasons [1]. Although their concentrations and spatial distribution can be deduced in experiments on excised tissue or sacrificed animals, there are many circumstances in which it is desirable to measure and image their concentrations *in vivo*. Magnetic resonance imaging (MRI) is based on the resonance of nuclei (typically protons, which are plentiful in biological tissues) with radiofrequency radiation in the presence of a static magnetic field [2]. Since the rate of precession of tissue protons is proportional to the local magnetic field strength, local fluctuations in field strength induced by the presence of magnetic nanoparticles can enhance the rate at which the transverse magnetisation of tissue protons decays with time [3, 4]. In many situations, magnetic nanoparticle concentrations in tissues are sufficiently high to be the main determinant of the tissue proton transverse relaxation rate (R_2), with higher concentrations resulting in higher values of tissue R_2 . The recent development of techniques for measuring and imaging R_2 in various biological tissues using

clinical magnetic resonance imagers makes such techniques readily available thus enabling measurement and imaging of magnetic nanoparticle concentrations once suitable calibration curves have been determined.

2. Pathological iron oxide nanoparticles

Iron overload disorders such as thalassaemia and hereditary haemochromatosis affect up to 0.5% of the world's population. These disorders result in the accumulation of iron in the form of nanoparticles of iron(III) oxyhydroxide in organs of the body such as the liver, heart, spleen, and pancreas. Knowledge of the concentrations of these particles is often essential for appropriate management of iron overload conditions. The currently accepted and widely used method of measurement is chemical analysis of needle biopsy specimens of the liver. However, needle biopsy is an invasive procedure that carries a degree of risk and has associated sampling errors owing to the uneven distribution of iron within tissues.

We have developed a method of measuring and imaging R_2 within the liver [5]. An example R_2 image of the liver is shown in figure 1. R_2 is highly dependent on tissue iron concentration owing to spin-spin interactions between protons of water molecules and the iron oxyhydroxide nanoparticles within the tissue. The high degree of correlation between R_2 and tissue iron concentration has enabled the development of a method for non-invasively measuring and imaging liver iron concentrations (figure 2) [6]. The method has a demonstrated dynamic range of measurement of liver iron concentration from 0.3 to 42.7 mg Fe/g dry liver tissue. The large dynamic range and sensitivity and specificity of liver R_2 to needle biopsy measurements together with a demonstrated high degree of reproducibility on multiple magnetic resonance imaging units offers readily available non-invasive absolute liver iron concentration measurements to the clinical community.

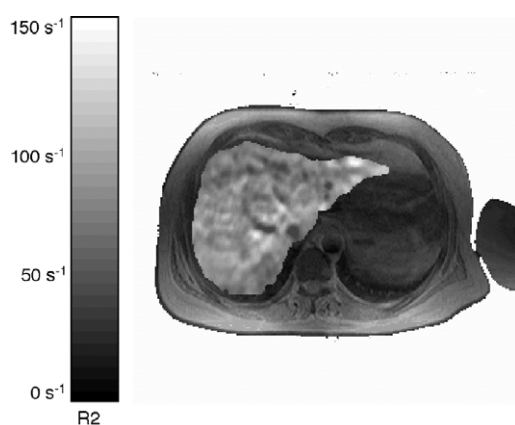


Figure 1. R_2 image of iron-loaded human liver. High R_2 corresponds to high iron concentration. The R_2 image of the liver is superimposed over a standard T_2 -weighted image. Note that T_2 is the proton transverse relaxation time ($T_2 = 1/R_2$).

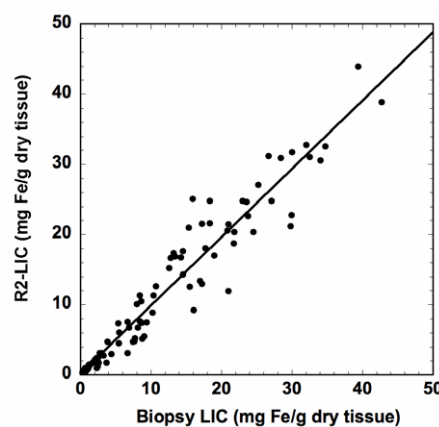


Figure 2. Correlation between liver iron concentration (LIC) measured *in vivo* using proton transverse relaxometry and LIC measured by needle biopsy in 105 human subjects (adapted from [6]).

Furthermore, there is promise that the ability to image liver iron concentrations may enable the detection of distorted liver architecture such as fibrosis and cirrhosis by virtue of the fact that these distortions result in altered patterns of iron oxyhydroxide nanoparticle deposition within the tissue (figure 3). Fibrosis and cirrhosis involve the proliferation of scar tissue within the liver. The scar tissue tends not to incorporate iron at the same concentrations as the liver cells and hence the presence of the scar tissue dilutes the macroscopic iron concentration in its vicinity [7].

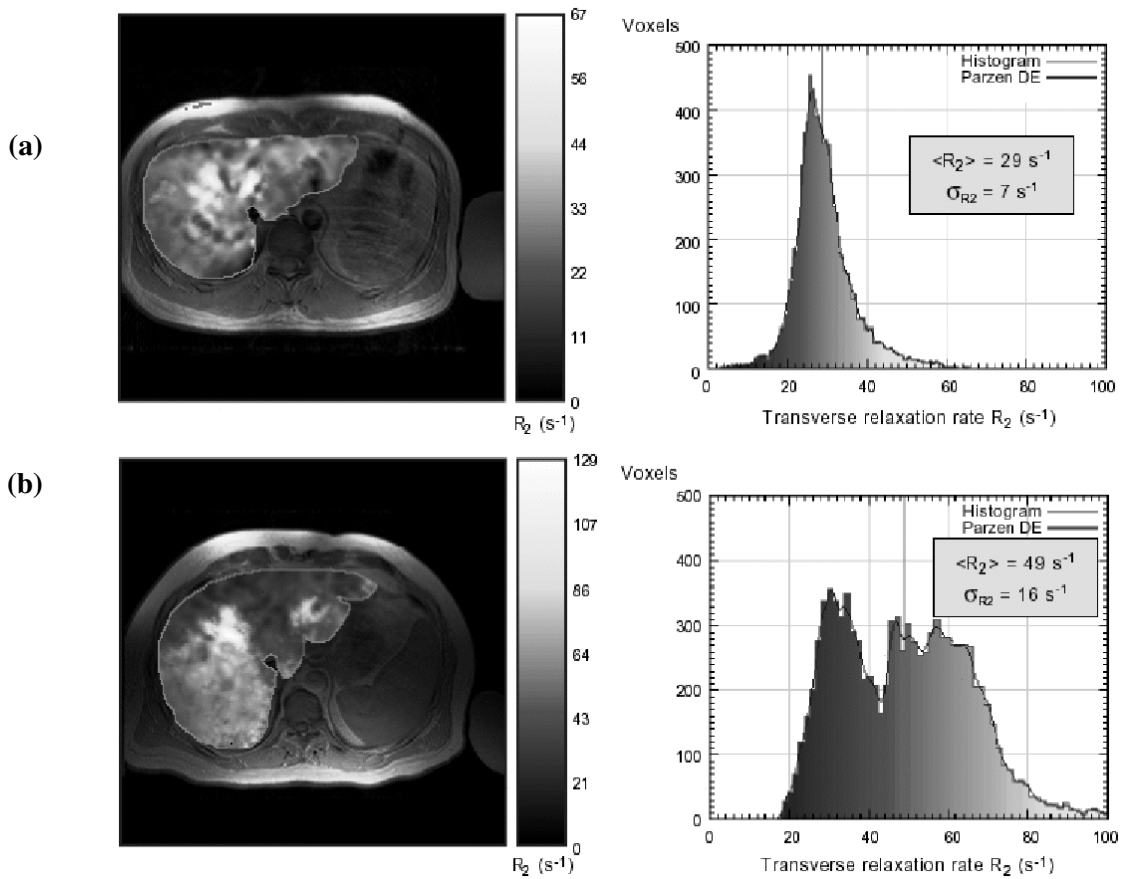


Figure 3. R_2 images of liver with corresponding R_2 distributions for two chronic hepatitis C patients. (a) patient with zero fibrosis score; (b) patient with cirrhosis (high fibrosis score). Note the distortion of the R_2 distribution away from normal for the patient with cirrhosis.

3. Magnetic particles for hyperthermia therapy

Mapping of tissue R_2 can also be used to image concentrations of magnetic particles introduced into the body such as those used for magnetic hyperthermia therapy [8, 9]. Magnetic hyperthermia therapy involves the application of alternating magnetic fields to tissues containing magnetic particles that have been targeted to tumour tissue in order to generate heat in the particles. Raised tissue temperatures can help to kill cancer cells and have been shown to increase the effectiveness of radio- and chemo-therapy. A safety concern of the technique is ensuring that the concentration of ferrimagnetic material in healthy parts of the liver is low enough to avoid unwanted heating of healthy liver tissue. Hence imaging of magnetic particle distributions *in vivo* may play a role in assessing the effectiveness of magnetic particle targeting of tumours before application of the ac magnetic field to heat the particles.

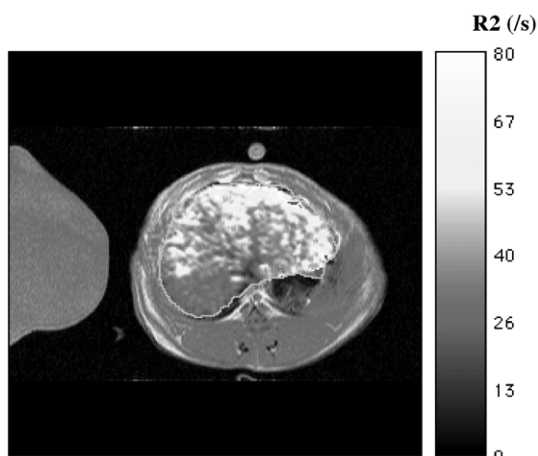


Figure 4. In vivo R_2 -image of rabbit liver embolized with ferrimagnetic iron particles (taken from [8]).

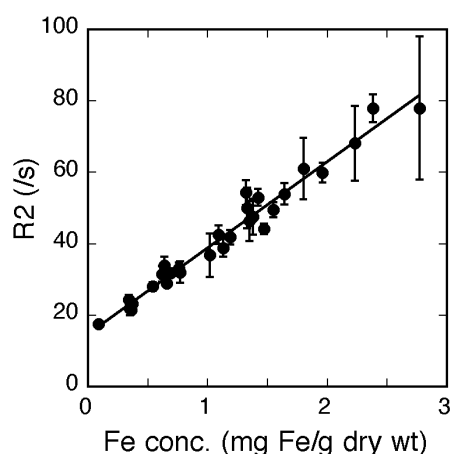


Figure 5. Graph of mean R_2 against iron concentration for approximate 1 cm cubes of tissue dissected from livers of rabbits loaded with ferrimagnetic particles (taken from [8]). Vertical bars through each data point indicate the width of the Gaussian distribution of R_2 observed for each sample of liver.

Figure 4 shows an R_2 image of a rabbit liver embolized with ferrimagnetic particles obtained *in vivo*. Figure 5 shows the calibration curve relating liver R_2 to concentration of the ferrimagnetic particles obtained by dissecting the excised liver into approximately 1 cm sized cubes post mortem and both chemically assaying for iron and measuring R_2 for each cube. Studies of heating rates and ferrimagnetic particle concentrations may lead to the R_2 images being used to predict local heating rates within the liver.

4. Ferrimagnetic particle detection limits

Since there are many situations where the concentrations of ferrimagnetic particles may be somewhat lower than those encountered in, for example, magnetic hyperthermia therapy, the limit of detection of ferrimagnetic particles by clinical magnetic resonance imaging systems has been investigated [10]. Such situations may include the use of nanoparticle “labels” within the human body. Magnetic nanoparticles functionalised with antigens for biomolecules of interest could be introduced into the body in order to magnetically label the biomolecules. Measurements on agar gels loaded with different concentrations of ferrimagnetic iron oxide nanoparticles indicate that ferrimagnetic iron concentrations as low as 50 $\mu\text{g/ml}$ can be measured and imaged [10]. Although this detection limit is not sufficiently low to enable measurement and imaging of the reported biogenic magnetite particle concentrations in the human brain [11, 12], the use of MRI microscopy systems with much higher field gradients than those available with clinical systems may aid in the study of these particles in excised human brain samples. MRI microscopy might also play a role in elucidating the distribution of magnetic particles in the geomagnetic sensory organs of animals capable of magnetic navigation.

5. References

- [1] Safarik I and Safarikova M 2002 Magnetic nanoparticles and biosciences *Monatshefte fur Chemie* **133** 737-59
- [2] Oppelt A and Grandke T 1993 Magnetic resonance imaging *Superconductor Science and Technology* **6** 381-95
- [3] Jensen J H and Chandra R 2002 Theory of nonexponential NMR signal decay in liver with iron overload or superparamagnetic iron oxide particles *Magn. Reson. Med.* **47** 1131-8

- [4] Gossuin Y, Roch A, Muller R N, Gillis P and Lo Bue F 2002 Anomalous nuclear magnetic relaxation of aqueous solutions of ferritin: An unprecedented first-order mechanism *Magn. Reson. Med.* **48** 959-64
- [5] St. Pierre T G, Clark P R and Chua-anusorn W 2004 Single spin-echo proton transverse relaxometry of iron loaded liver *NMR in Biomedicine* **17** 446-58
- [6] St. Pierre T G, Clark P R, Chua-anusorn W, Fleming A J, Jeffrey G P, Olynyk J K, Pootrakul P, Robins E and Lindeman R 2005 Noninvasive measurement and imaging of liver iron concentrations using proton magnetic resonance *Blood*. **105** 855-61
- [7] Clark P R, Chua-anusorn W and St Pierre T G 2003 Proton transverse relaxation rate (R2) images of iron-loaded liver tissue: Mapping local tissue iron concentrations with MRI *Magn. Reson. Med.* **49** 572-5
- [8] Pardoe H, Clark P R, St Pierre T G, Moroz P and Jones S K 2003 A magnetic resonance imaging based method for measurement of tissue iron concentration in liver arterially embolized with ferrimagnetic particles designed for magnetic hyperthermia treatment of tumors *Magn. Reson. Imaging* **21** 483-8
- [9] Moroz P, Pardoe H, Jones S K, St Pierre T G, Song S and Gray B N 2002 Arterial embolization hyperthermia: hepatic iron particle distribution and its potential determination by magnetic resonance imaging *Phys. Med. Biol.* **47** 1591-602
- [10] Pardoe H, Chua-anusorn W, St. Pierre T G and Dobson J 2003 Detection limits for ferrimagnetic particle concentrations using magnetic resonance imaging based proton transverse relaxation rate measurements *Phys. Med. Biol.* **48** N89-N96
- [11] Kirschvink J L, Kobayashi-Kirschvink A and Woodford B J 1992 Magnetite biomineralization in the human brain *Proc. Nat. Acad. Sci.* **89** 7683-7
- [12] Dobson J 2002 Investigation of age-related variations in biogenic magnetite levels in the human hippocampus *Exp. Brain Res.* **144** 122-6